Hydrophobic Metal Organic Framework Enhanced Acoustic Wave Formaldehyde Sensor Based on Polyethyleneimine and Bacterial Cellulose Nanofilms

J.L. Wang (993553580@qq.com)
University of Electronic Science and Technology of China https://orcid.org/0000-0002-1444-0838

J.H. Shang
Hefei University of Technology

Y.J. Guo
University of Electronic Science and Technology of China

Y.Y. Jiang
Fudan University

W.K. Xiong
University of Electronic Science and Technology of China

J.S. Li
China Academy of Engineering Physics

X. Yang
China Academy of Engineering Physics

H. Torun
University of Northumbria at Newcastle: Northumbria University

Y.Q. Fu
University of Northumbria at Newcastle: Northumbria University

X.T. Zu
University of Electronic Science and Technology of China

Research Article

Keywords: Hydrophobicity, Formaldehyde gas sensor, Zeolitic imidazolate framework-8 (ZIF-8), Polyethyleneimine (PEI), Bacterial cellulose (BC)

Posted Date: March 22nd, 2021

DOI: https://doi.org/10.21203/rs.3.rs-312460/v1

Version of Record: A version of this preprint was published at Journal of Materials Science: Materials in Electronics on July 7th, 2021. See the published version at https://doi.org/10.1007/s10854-021-06241-6.

Abstract

A surface acoustic wave (SAW) formaldehyde gas sensor was fabricated on a 42°75' ST-cut quartz substrate, with a composite sensing layer of zeolitic imidazolate framework (ZIF)-8 on polyethyleneimine (PEI)/ bacterial cellulose (BC) nanofilms. The addition of snowflake-like ZIF-8 structure on the PEI/BC sensitive film significantly improves the hydrophobicity of the SAW sensor and increases the sensor's sensitivity to formaldehyde gas. It also significantly increases the surface roughness of the sensitive film. Its hydrophobic nature prevents water molecules from entering into the internal pores of the BC film, thereby avoiding significant mass loading caused by the humidity change when the sensor is used to detect low-concentration formaldehyde gas. The Zn^{2+} sites at the surface of ZIF-8 improves the sensor's response to formaldehyde gas through enhancing the physical adsorptions. Experimental results show that the ZIF-8@PEI/BC SAW sensor has a response (e.g., frequency shift) of 40.3 kHz to 10 ppm formaldehyde gas at 25℃ and 30% RH. When the relative humidity was increased from 30% to 93%, the response (frequency shift) of the sensor drifts only ~5%, and there is negligible drift at a medium humidity level (~56% RH).

1. Introduction

With the rapid growth of economy and increasing demand for comfortable living environment, decoration materials are extensively used in the built environment, which brings complex and diverse pollutants including formaldehyde into the indoor environment [1, 2]. Among various types of air pollutants, formaldehyde has received significant attention because of its wide usage and toxicity. Being a reactive compound, formaldehyde can damage proteins, cause genetic mutations, DNA single-strand internal cross-linking and DNA-protein cross-linking, and inhibit DNA damage repair, etc. [3]. Long-term exposure to low-dose formaldehyde can cause chronic respiratory diseases, nasopharyngeal cancer, brain tumors and other diseases [4, 5]. Therefore, a timely and precise detection of formaldehyde concentration is particularly important.

Many types of formaldehyde detection methods, such as spectrophotometry, chromatography, and fluorescence spectroscopy, have been proposed. [6–8]. However, they are generally expensive, and often require a long cycle of sampling and analysis operated by professionals. The measurement results using these methods are usually the mean values over a period of time, which does not reflect the formaldehyde concentration in real time [9].

Up to now, the research of formaldehyde gas sensor is mostly focused on the development of detection techniques, which require both high sensitivity and short detection period, in the air in real time [10]. For example, Bouchikhi et al. developed a metal oxide thin film-based sensor by vapor deposition of tungsten trioxide (WO_3) nanowires (NWs) and metal nanoparticles modified WO_3 NWs gas sensing layer on interdigital platinum electrode, and the sensor showed a high sensitivity for formaldehyde gas under both dark and ultraviolet light irradiation conditions [11]. Yin et al developed a polymer thin film sensor by applying a flower-like compound with a heterostructure based on Sn_3O_4 and reduced graphene oxide

(rGO) to achieve a wide detection range of formaldehyde gas [12]. These types of sensors have the advantages of high sensitivity and low detection limit. However, they often suffer from the severe interferences of temperature and humidity changes. Up to now, there are not many studies to minimize the interferences of temperature and humidity. For example, Wang et al. proposed a formaldehyde gas sensor based on Cu-doped Sn_3O_4 nanoflowers [13]. Its response to 100 ppm formaldehyde is 53 (the ratio of the resistances of the sensor in dry air and the gaseous environment), with a detection limit of 1 ppm, but the changes of humidity have a significant impact on the detection results. An offset of about 10% in response is reported between 25% and 75% RH environments [13]. Zeng et al. prepared a La_2O_3-In_2O_3 and nanotube sensor using an electrospinning method, and the sensor has a response value of 101.9 to 50 ppm formaldehyde gas. They reported that when the RH value was lower than 60%, the sensor's response to formaldehyde gas was relatively stable, but when the RH value was higher than 60%, the sensor's response to formaldehyde gas was decreased sharply with the increase of RH values [14].

Previously, we developed a surface acoustic wave (SAW) formaldehyde gas sensor based on a bi-layer nanofilm of bacterial cellulose (BC) and polyethyleneimine (PEI) [15]. The BC nano layer significantly improves the sensitivity of the PEI film and reduces the response and recovery time for the low concentrations of formaldehyde. The sensor has a frequency shift of 35.6 kHz to 10 ppm formaldehyde gas at room temperature and 30% relative humidity (RH), with both good selectivity and stability. The sensor uses a ST-cut quartz substrate which has a low temperature coefficient of frequency (TCF). However, it shows a poor performance with the change of humidity, because the amine groups of PEI and the hydroxyl groups of BC have strong adsorptions of H_2O molecules [16, 17], thus causing a significant mass loading effect of the SAW sensor. One way to solve this problem is to install a humidity sensor next to this formaldehyde SAW sensor which can quantitatively detect humidity to correct the SAW sensor output through offline data analysis. However, this is an indirect compensation increasing the complexity, size and production cost of the formaldehyde sensor. Therefore, under the premise of maintaining the PEI/BC sensing film's sensing performance for formaldehyde gas, solving the problem of its high sensitivity to RH values becomes our key research topic to improve the performance of the formaldehyde gas sensor.

Changes of hydrophobicity is currently a research hotspot in the field of functional materials [18]. It is also important in the field of gas sensing, and a high hydrophobic layer on the top of the sensor can prevent the sensor from interfering with the changes of environmental humidity [19]. The hydrophobic layer can prevent water molecules from easily entering the sensitive film, thereby reducing the frequency shift of the mass loading caused by the water molecules in the formaldehyde gas detection process. Recently, researchers have applied various methods to improve the hydrophobicity of sensors. For example, Lee et al. used an ultrafiltration method to successfully exchange water-based poly-(3,4-ethylenedioxythiophene) polystyrene sulfonate (PEDOT: PSS) solution to organic solvent-based PEDOT: PSS solution, which was applied as a coating on a pressure sensor to increase the contact angle of water droplets and avoid the influence of humidity changes to sensors [20]. Chen et al. used a hydrophobic cysteine-sensitized Cu_2O(Cu(I)-Cys) nanocomposite as a sensing layer to fabricate a quartz microbalance

gas sensor, which could determine hexanal and 1-octen-3-ol at room temperature, with a good hydrophobicity, sensitivity and selectivity [21].

Zeolite-based imidazole salt frameworks (ZIFs) are a type of metal organic frameworks (MOFs), which are porous crystalline materials formed by continuous and periodic connection of transition metal ions and imidazole-based organic linkers [22, 23]. Due to its high porosity, thermal/chemical stability, surface functionality and diverse synthesis methods, ZIFs have been widely used in various fields, including gas storage, catalysis, and preparation of various nanostructures [24–26]. Li et al [27] and Yogapriya et al. [28] reported that the ZIFs have good hydrophobic properties (high water contact angle), and its hydrophobic properties can be further improved by compounding with other materials such as polyvinylidene fluoride or porous fluorinated graphene. The ZIF-8 is regarded as having the best hydrophobic properties among all the ZIF materials [29]. In this study, we proposed to use MOF ZIF-8 structure to improve the humidity insensitivity of the PEI/BC nanofilms SAW formaldehyde gas sensor. We found that the contact angle of a water droplet on the sensing layer can reach ~ 135°, showing its high hydrophobicity. We also found that the creation of many metal ion (Zn^{2+}) sites on the porous surface of the sensor improves the sensor's response to formaldehyde gas through effective physical adsorptions [30].

2. Experimental Details

2.1 SAW resonator and composite nano sensing layer

Surface acoustic wave resonator (SAWR) was made on a quartz substrate (12 mm × 3 mm × 0.5 mm, ST-cut type of 42°75' y-axis rotary cutting) with a TCF value of 0.24 ppm/°C [31]. Al electrode interdigital transducers (IDTs, 30 pairs) and reflective gratings (100 pairs) were deposited on the quartz substrate. IDTs have a finger width and spacing of 4 μm and an aperture of 3 mm. The reflection grating has the same structure and dimension as the IDTs, both of which are shown in Fig. 1. The resonant frequency of the designed SAWR is ~ 200 MHz. In order to prevent the growth of sensitive materials in the IDTs and their reflectors during the subsequent processes, we used a polyimide tape to cover most of SAWR area except the sensing region.

The hydrophobic composite sensing layer uses BC film as the structural substrate, PEI particles to provide reaction sites, and ZIF-8 shell as the hydrophobic layer. The fermentation process of BC solution and the preparation process of PEI/BC bi-layer films have been introduced in detail in our previous work [15]. The BC hydrosol (1 wt‰) and PEI hydrosol (1.25 wt‰) were sequentially coated onto the ST-cut quartz substrate with the spinning speeds of 6000 and 7000 rpm, respectively, then dried in an oven at 60℃ for 10 minutes to make a PEI/BC bi-layer on the SAWR. For synthesis of ZIF-8, 2-methylimidazole (MIN) was used as a linking agent. The molar ratio of the synthesis solution was Zn^{2+}:MIN:H_2O = 1:8:1000. Firstly, 3.28 g MIN was dissolved in 60 mL deionized water. Then, 1.96 g $Zn(NO_3)_2{\cdot}6H_2O$ was dissolved in 30 mL deionized water. Finally, the zinc nitrate solution was mixed with the MIN solution under a constant stirring process. Zinc nitrate and MIN were obtained from Shanghai Aladdin Biochemical Technology Co.,

Ltd, China. All the preparation steps were carried out at room temperature (25°C). The top side of SAWR coated with PEI/BC bi-layer nanofilms was gently put into the synthesis solution, which was placed in a constant temperature reactor at 60°C for 8 hours. After this, the SAWR with the composite sensing layer was thoroughly cleaned with methanol and deionized water to remove any physically adsorbed ZIF-8 crystals and unreacted precursors. After cleaning, the SAWR was placed in an oven at 60℃ for 10 minutes to obtain the SAWR with the ZIF-8@PEI/BC composite nanofilm. The PEI/BC bi-layer nanofilms without applied with the MIM solution, and a PEI film which was soaked in the MIM solution were used as the control groups for comparisons. Finally, the SAWRs coated with the sensing films were connected to oscillator-based readout circuits (including amplification and phase shifting) by spot welding using gold wires to form a SAW based formaldehyde gas sensor.

2.2 Sensing and characterization system

The experimental sensing system is illustrated in Fig. 2. The temperature and humidity of the laboratory environment were controlled at 25°C and 30% RH, respectively. The sensing system includes two enclosed chambers of 2 L inside and 20 L outside, a workbench with the constantly controlled temperature, evaporation station, saturated salt solution bottle, thermometer, hygrometer, frequency counter, and digital source meter. The 2 L testing chamber was placed inside the 20 L testing chamber, and the SAW device was kept inside the 2 L testing chamber. Formaldehyde solution was dropped on the evaporation station using a micropipette in the 20 L test chamber. The relative humidity control was implemented using a humidifier and the flowing dried N_2 gas. After the formaldehyde solution evaporates, the power supply of the evaporator was disconnected and test chamber was returned back to room temperature of 25°C. A digital source meter and frequency counter were then switched on so that the output frequency of the SAW device is stabilized. Then the 2 L test chamber was slowly opened through a mechanical pulley to introduce the formaldehyde gas to the surface of the SAW gas sensor. The output frequency deviation of SAWR gas sensor was continuously monitored using a frequency counter (Agilent 53210A). Based on our previous work, the volume V_{liquid} of the formaldehyde solution required to set the concentration of formaldehyde gas can be obtained using Eq. 1 [15],

$$V_{liquid} = 6.758 \bullet \frac{C}{T} \qquad (1)$$

where C (ppm) is the required concentration of formaldehyde gas, and T (K) is the temperature of the test environment. A field emission scanning electron microscope (FE-SEM, FEI-INSPECT F50) was used to characterize the surface morphology of the sensing film. A Kruss G10 Drop Shape Analyzer Goniometer was employed to measure the water contact angle on the ZIF-8@PEI/BC composite nanofilm. The contact angle values reported were an average of three separate measurements carried out at three different locations on the film surface.

3. Results And Discussions

3.1 Morphological characterization of sensing film

Figure 3 shows the SEM images of PEI film, PEI/BC bi-layer nanofilms and ZIF-8@PEI/BC composite nanofilms. Due to the high viscosity and small particle size of PEI colloids, the surface of the PEI film shows some uneven agglomerates without obvious large pores. The PEI/BC bi-layer nanofilms inherit the porous and fibrous network structure of the BC film, and the PEI particles are evenly distributed on the surface of the BC film. For the ZIF-8@PEI/BC composite nanofilms, a snowflake-like structure of zeolite imidazole metal salt framework can be seen formed in the sensing area of the resonator. This snowflake-like structure increases the roughness of the sensitive film and increases the contact angle of water droplets on the film [32]. The hydrophobic ZIF-8 structure prevents water molecules from entering the BC pores, thereby reducing the frequency shift of the mass loading caused by the water molecules in the formaldehyde gas detection process.

3.2 Gas sensing detection and sensing mechanism

Figure 4 shows the response frequency of SAW sensors coated with ZIF-8@PEI nanofilms, PEI/BC bi-layer nanofilms, and ZIF-8@PEI/BC composite nanofilms when exposed to 10 ppm formaldehyde gas in 30% RH environment. All three types of sensors respond well, which is due to the reversible nucleophilic reactions between formaldehyde molecules and PEI at room temperature [33]. The response mechanism of PEI adsorbing formaldehyde molecules is shown in Fig. 5. The electron pairs of the polar double bonds for the formaldehyde molecules are transferred to the oxygen atoms, thus the oxygen atom is negatively charged, and the carbon atom is positively charged. This makes the carbon atoms becoming electrophilic. However, there is a lone pair of electrons in the nitrogen atom of the amine group, which is easy to be used as a nucleophile to attack the electrophile. This causes a nucleophilic reaction. The two bonds in the formaldehyde molecules are broken, thus forming two new covalent bonds. The formaldehyde molecules are then adsorbed by the sensing layer, thus causing a mass loading of the SAW sensor.

The frequency responses of SAW sensors coated with ZIF-8@PEI/BC films and PEI/BC films to 10 ppm formaldehyde gas are much larger than that coated with ZIF-8@PEI. This can be attributed to the porous network structure of the BC nanofiber film facilitating more sites for the absorption of formaldehyde gas molecules. The hydrogen bonds formed between the hydroxyl group on the surface of BC and the amine group of PEI prevent the aggregation of PEI particles, which ensure the uniform distribution of PEI on the BC film and enhance the adsorption of formaldehyde gas molecules. This has been reported in our previous work [15]. In addition, for 10 ppm formaldehyde gas, the frequency shift of the SAW sensor coated with ZIF-8@PEI/BC films is 13% higher than that of PEI/BC films. This is because the Zn^{2+} sites provide extra physical adsorption positions for the formaldehyde molecules. Each Zn^{2+} ion on the surface of ZIF-8 can adsorb one formaldehyde molecule, and all the Zn ions on the surface can adsorb formaldehyde molecules simultaneously. When there are many formaldehyde molecules in the chamber, the formaldehyde molecules are preferentially adsorbed on the surface of Zn^{2+} ions. After the formaldehyde molecules are covered the Zn^{2+} surfaces, the remaining formaldehyde molecules can be

weakly connected with the those already adsorbed on the Zn^{2+} surface. For more details of the adsorption mechanism of Zn^{2+} sites on formaldehyde molecules, the readers can refer to the work reported by Chen et al using a density functional theory [30]. Our study reveals that the presence of the ZIF-8 metal framework enhances the response of the sensitive film to formaldehyde gas.

Figure 6 showed the response dynamic curves of SAW sensors based on ZIF-8@PEI/BC composite nanofilm, PEI/BC film and ZIF-8@PEI film, when exposed to different concentrations of formaldehyde gas from 100 ppb to 10 ppm at 25°C and 30% RH. The response curves clearly show that the presence of ZIF-8 enhances the sensor's response to formaldehyde gas. The sensor also shows good stability to formaldehyde gas, as there is no apparent baseline drift.

The response time of the sensor is defined as the time required to reduce the resonant frequency to 90% of the maximum frequency shift, and the recovery time is the time required to restore the resonant frequency to 10% of the maximum frequency shift. Figure 7 shows the typical response and recovery characteristic curves of SAW sensors with ZIF-8@PEI/BC composite nanofilm and PEI/BC film, when exposed to 10 ppm formaldehyde gas in the test chamber environment at 25°C and 30% RH. Even though there is an added ZIF-8 layer, the response time and recovery time of the SAW sensor are only slightly increased, which does not show significant effect on the overall sensing performance. This may be due to the fact that the ZIF metal framework can significantly increase the specific surface area of the sensitive membrane and does not reduce the effective transport and adsorption of gas molecules.

3.3 Detection and mechanism of hydrophobicity

Figure 8(a) shows the repeated response recovery curves of SAW sensors, coated with PEI/BC film, ZIF-8@PEI film and ZIF-8@PEI/BC composite nanofilm, when exposed to 10 ppm formaldehyde gas in different chamber environments with relative humidity values of 30%, 56% and 84%, respectively. The responses of PEI/BC films SAW sensor to 10 ppm formaldehyde gas are increased with the increase of relative humidity levels. This is because the amine group of PEI and the hydroxyl group of BC have strong attractions to H_2O molecules, which increases the mass loading of the SAW sensor. The frequency shifts of SAW sensors with ZIF-8@PEI film and ZIF-8@PEI/BC composite nanofilm to 10 ppm formaldehyde gas show little changes with the humidity levels, and the sensors show good responses in different RH environments, with response drifts less than 3%. Figure 8(b) shows the frequency shift of three SAW sensors exposed to 10 ppm formaldehyde gas under different relative humidity levels between 43%~93%. Compared with the low humidity (10% RH) environment, the PEI/BC bi-layer nanofilms SAW sensor without growth the ZIF-8 has a nearly 50% drift in the frequency response to 10 ppm formaldehyde gas under a high humidity (93% RH) environment. Humidity changes have considerable impact on the sensor's response to formaldehyde. The frequency response of ZIF-8@PEI and ZIF-8@PEI/BC composite nanofilms SAW sensors to 10 ppm formaldehyde gas has a response drift of less than 5% under these two types of humidity (10% RH and 93% RH). This shows that the influence of humidity on the concentration of formaldehyde has been greatly reduced. Therefore, it is confirmed that the presence of ZIF-8 makes the SAW sensor much less sensitive to humidity.

In order to verify that the growth of ZIF-8 improves the hydrophobic performance of the sensing film, we measured contact angles of water droplets placed on the film surface. As shown in Fig. 9(a), the PEI/BC films are hydrophilic with a contact angle is ~ 20° due to the strong hydrogen bonds formed between the amine group of PEI and the hydroxyl group of BC. The addition of ZIF-8 increases the contact angle of the ZIF-8@PEI/BC composite nanofilms to 135°, as shown in Fig. 9(b). This is attributed to the fact that the growth of ZIF-8 crystals with a snowflake flake structure significantly increases the surface roughness (R_f) of the sensing layer. As is well reported, the hydrophobicity and surface roughness of the film are the two main factors which affect the water contact angle value of the surface [32, 34]. When water droplets are placed on the rough surface of the film, the following equation is normally used to predict the water contact angle [35]:

$$\cos\theta_\omega = R_f \cos\theta_0 \qquad (2)$$

where θ_ω and θ_0 are the contact angles of water droplets on the rough film surface and the smooth film surface, respectively. R_f is a dimensionless factor, equal to the ratio of the surface area to its flat projected area. Accordingly, the contact angle of water droplets on the rough hydrophobic film surface is much larger than that on the smooth surface. This means that the hydrophobic properties of the film will increase with the increase of R_f. Therefore, ZIF-8 with snowflake-like structure greatly improves the hydrophobicity of the sensitive film. The hydrophobic ZIF-8 structure prevents water molecules from entering the internal pores of the BC membrane, and avoids the frequency shift of the sensor's mass loading caused by the change of environmental humidity when the sensor detects low-concentration formaldehyde gas.

3.4 Stability and selectivity of SAW sensors

In order to characterize the sensor response with respect to temperature changes, we measured its resonance frequency in a temperature range of 25–60℃. Figure 10(a) shows that as the temperature increases, the resonant frequency of the sensor decreases slightly. The changes of resonant frequency show a good linear relationship with the temperature change. The TCF of the SAW sensor coated with ZIF-8@PEI/BC composite nanofilms is -0.24 ppm/℃. This level shows the sensor response is not affected by temperature in practical gas sensing conditions.

The SAW sensor coated with ZIF-8@PEI/BC composite nanofilms were repeatedly tested with the formaldehyde for every 5 days by exposing to 100 ppb-10 ppm formaldehyde gas. The responses (or frequency shifts) were recorded for 40 days to test its long-term stability. The results are shown in Fig. 10(b). The fluctuation of the frequency shift of the sensor is less than 5%, and there is almost no fluctuation at low concentrations, indicating that the sensor has a good long-term stability.

We further tested the selectivity of the SAW sensor with the ZIF-8@PEI/BC composite nanofilms to different types of commonly used gases, including 100 ppm reducing gases CO, H_2, NH_3, H_2S, and oxidizing gases NO_2, volatile gases ethanol, benzene, toluene, etc., and 10 ppm of target gas

formaldehyde. The frequency response tests were carried out separately, and the results are shown in Fig. 10(c). Similar to the results of the PEI/BC bi-layer nanofilms SAW sensor reported in Ref. [15], the frequency shifts of CO, H_2, NH_3, H_2S, NO_2, benzene, and toluene remain almost unchanged. The SAW sensor coated with ZIF-8@PEI/BC composite nanofilms has almost no response to ethanol gas, whereas that coated with PEI/BC bi-layer nanofilms has a slight deviation in response to ethanol gas. This may be due to the improved hydrophobic properties of the ZIF-8@PEI/BC composite nanofilms, which prevents water molecules from entering the internal pores of the film, thereby reducing the adsorption of ethanol gas by water molecules. Therefore, compared with the response of 40.3 kHz of the formaldehyde gas, the response of non-target gases at low concentrations is weak and negligible, which indicates that the sensor has a good selectivity to formaldehyde gas.

4. Conclusions

In summary, we report that snowflake-like structure of MOF ZIF-8 coated on SAW resonator can improve the hydrophobic properties of PEI/BC bi-layer nanofilms, and enhance the sensor's sensitivity to formaldehyde gas. The snowflake ZIF-8 structure significantly increases the surface roughness of the sensitive film and defining a hydrophobic sensing layer. The hydrophobic ZIF-8 structure prevents water molecules from entering the internal pores of the BC film, and avoids the mass loading change caused by the environmental humidity change when the sensor detects low-concentration formaldehyde gas. The experimental results show that the response of the SAW sensors with ZIF-8@PEI/BC composite nanofilms exposed to 10 ppm formaldehyde gas has a drift of less than 5% in an environment where the RH changes between 10% and 93%. This is a significant improvement over SAW sensors with PEI/BC bi-layer nanofilms that exhibit 50% frequency drift within the same RH variation. In addition, the Zn^{2+} sites on the surface of ZIF-8 further improve the sensor's response to formaldehyde gas through physical adsorption. The SAW sensor coated with ZIF-8@PEI/BC composite nanofilms also has good selectivity and long-term stability to the targeted formaldehyde gases.

Declarations

Acknowledgments

This study was supported financially by the Fundamental Research Funds for the Central Universities (No. A03018023801119), the Joint Fund of the National Natural Science Foundation of China and the China Academy of Engineering Physics (Grant No. U1930205), Engineering Physics and Science Research Council of UK (EPSRC EP/P018998/1) and UK Fluidic Network-Special Interest Group of Acoustofluidics, and Newton Mobility Grant (IE161019) through Royal Society and NFSC, and Royal Academy of Engineering: Research Exchange between UK and China.

References

1. H. Chen, L. Sun, G. Li, X. Zou, Well-tuned surface oxygen chemistry of cation off-stoichiometric spinel oxides for highly selective and sensitive formaldehyde detection. Chem. Mater. **30**, 2018–2027 (2018)
2. Lv, Pin, Study on key detecting technologies for indoor air quality controlling, Dalian University of Technology 2008
3. X. Wang, B. Ding, M. Sun, M.J.Y. Yu, G. Sun, Nanofibrous polyethyleneimine membranes as sensitive coatings for quartz crystal microbalance-based formaldehyde sensors. Sens. Actuators B **144**, 11–17 (2010)
4. P.R. Chung, C.T. Tzeng, M.T. Ke, C.Y. Lee, Formaldehyde Gas Sensors: A Review, Sensors **13**, 4468–4484 (2013)
5. A. Allouch, M. Guglielmino, P. Bernhardt, C.A. Serra, S. Le Calve, Transportable, fast and high sensitive near real-time analyzers: Formaldehyde detection. Sens. Actuators B **181**, 551–558 (2013)
6. Y.Y. Xie, Determination of microscale formaldehyde in wastewater by AHMT spectrophotometry, Technol. Dev. Chem. Ind. **16**, 49–51 (2013)
7. B.K. Ma, F.J. Xu, M. He, Y.Q. Lin, G.H. Hu, M. Zhang, X.Y. Zhao, W.L. Liu, Detection of residual formaldehyde in N-butyl-2-cyanoacrylate by high-performance liquid chromatography with rhodamine B hydrazide. Microchem. J **158**, 105222 (2020)
8. Y. Du, H.O. Qiu, M. Shao, Determination of formaldehyde in air by method of acetylacetone with fluorescence. Saf. Environ. Eng. **18**, 42–46 (2011)
9. X. Liu, Y. Zhang, X. Yang, Vitamin E reduces the extent of mouse brain damage induced by combined exposure to formaldehyde and PM 2.5, Ecotoxicol. Environ. Saf. **172**, 33–39 (2019)
10. L.Y. Wang, Y.P. Yu, Q. Xiang, J. Xu, Z.X. Cheng, J.Q. Xu, PODS-covered PDA film based formaldehyde sensor for avoiding humidity false response. Sens. Actuators B **255**, 2704–2712 (2018)
11. B. Bouchikhi, T. Chludzinski, T. Saidi, J. Smulko, N.El Bari, H. Wen, R. Ionescu, Formaldehyde detection with chemical gas sensors based on WO_3 nanowires decorated with metal nanoparticles under dark conditions and UV light irradiation, Sens. Actuators B 320 (2020)
12. F.F. Yin, Y. Li, W.J. Yue, S. Gao, C.W. Zhang, Z.X. Chen, Sn_3O_4/rGO heterostructure as a material for formaldehyde gas sensor with a wide detecting range and low operating temperature, Sens. Actuators B 312 (2020)
13. L. Wang, Y. Li, W.J. Yue, S. Gao, C.W. Zhang, Z.X. Chen, High-performance formaldehyde gas sensor based on Cu-doped Sn_3O_4 hierarchical nanoflowers. IEEE Sens. J. **20**, 6945–6953 (2020)
14. X.G. Zeng, L. Liu, Y.F. Lv, B. Zhao, X.N. Ju, S.Y. Xu, J.X. Zhang, C.X. Tian, D. Sun, X.N. Tang, Ultra-sensitive and fast response formaldehyde sensor based on La_2O_3-In_2O_3 beaded nanotubes at low temperature, Chem. Phys. Lett. 746 (2020)
15. J.L. Wang, Y.J. Guo, G.D. Long, Y.L. Tang, Q.B. Tang, X.T. Zu, J.Y. Ma, B. Du, H. Torun, Y.Q. Fu, Integrated sensing layer of bacterial cellulose and polyethyleneimine to achieve high sensitivity of ST-cut quartz surface acoustic wave formaldehyde gas sensor. J. Hazard. Mater. **388**, 121743 (2020)

16. Z. Yuan, H.L. Tai, Y.J. Su, G.Z. Xie, X.S. Du, Y.D. Jiang, Self-assembled graphene oxide/polyethyleneimine films as high-performance quartz crystal microbalance humidity sensors, Rare Met. 13 (2020)
17. J.L. Wang, Y.J. Guo, D.J. Li, G.D. Long, Q.B. Tang, X.T. Zu, J.Y. Ma, B. Du, Y.L. Tang, H. Torun, Y.Q. Fu, Bacterial cellulose coated ST-cut quartz surface acoustic wave humidity sensor with high sensitivity, fast response and recovery. Smart Mater. Struct. **29**, 045037 (2020)
18. L. Xie, D.L. Yang, Q.Y. Lu, H. Zhang, H.B. Zeng, Role of molecular architecture in the modulation of hydrophobic interactions. Curr. Opin. Colloid Interface Sci. **47**, 58–69 (2020)
19. S. Shiba, K. Yamada, M. Matsuguchi, Humidity-resistive optical NO gas sensor devices based on cobalt tetraphenylporphyrin dispersed in hydrophobic polymer matrix, Sensors 20 (2020)
20. J.J. Lee, S. Gandla, B. Lim, S. Kang, S. Kim, S. Lee, S. Kim, Alcohol-based highly conductive polymer for conformal nanocoatings on hydrophobic surfaces toward a highly sensitive and stable pressure sensor. NPG Asia Mater. **12**, 1 (2020)
21. W. Chen, Z.H. Wang, S. Gu, J. Wang, Y.W. Wang, Z.B. Wei, Detection of hexanal and 1-octen-3-ol in refrigerated grass carp fillets using a QCM gas sensor based on hydrophobic Cu(I)-Cys nanocomposite, Sens. Actuators B 305 (2020)
22. A. Phan, C.J. Doonan, F.J. Uribe-Romo, C.B. Knobler, M. O' Keeffe, O.M. Yaghi, Synthesis, structure, and carbon dioxide capture properties of zeolitic imidazolate frameworks. Acc. Chem. Res. **43**, 58–67 (2010)
23. B.R. Pimentel, A. Parulkar, E.K. Zhou, N.A. Brunelli, R.P. Lively, Zeolitic imidazolate frameworks: next-generation materials for energy-efficient gas separations. ChemSusChem **7**, 3202–3240 (2014)
24. S.B. Wang, X.C. Wang, Imidazolium ionic liquids, imidazolylidene-heterocyclic carbenes, and zeolitic imidazolate frameworks for CO_2 capture and photochemical reduction. Angew. Chem. Int. Ed. **55**, 2308–2320 (2016)
25. K. Liang, J.J. Richardson, J. Cui, F. Caruso, C.J. Doonan, P. Falcaro, Metal-organic framework coatings as cytoprotective exoskeletons for living cells. Adv. Mater. **28**, 7910–7914 (2016)
26. D. Kim, D.W. Kim, W.G. Hong, A. Coskun, Graphene/ZIF-8 composites with tunable hierarchical porosity and electrical conductivity. J. Mater. Chem. A **4**, 7710–7717 (2016)
27. H.B. Li, H.J. Liu, W.Y. Shi, H.X. Zhang, R. Zhou, X.H. Qin, Preparation of hydrophobic zeolitic imidazolate framework-71 (ZIF-71)/PVDF hollow fiber composite membrane for membrane distillation through dilute solution coating, Sep. Purif. Technol. 251 (2020)
28. R. Yogapriya, K.K.R. Datta, Porous fluorinated graphene and ZIF-67 composites with hydrophobic-oleophilic properties towards oil and organic solvent sorption. J. Nanosci. Nanotechnol. **20**, 2930–2938 (2020)
29. E.E. Sann, Y. Pan, Z.F. Gao, S.S. Zhan, F. Xia, Highly hydrophobic ZIF-8 particles and application for oil-water separation. Sep. Purif. Technol. **206**, 186–191 (2018)

30. D. Chen, Y.J. Yuan, Thin-film sensors for detection of formaldehyde: A review. IEEE Sens. J. **15**, 6749–67602 (2015)
31. J. Devkota, P. Jagannath, D. Ohodnicki, SAW sensors for chemical vapors and gases. Sensors **17**, 801 (2017)
32. L. Feng, C. Musto, K. Suslick, A simple and highly sensitive colorimetric detection method for gaseous formaldehyde. J. Am. Chem. Soc. **132**, 4046–4047 (2010)
33. Y. Liao, R. Wang, G.F. Anthony, Engineering superhydrophobic surface on poly(vinylidene fluoride) nanofiber membranes for direct contact membrane distillation. J. Membr. Sci. **440**, 77–87 (2013)
34. Y.H. Zhao, B.K. Zhu, L. Kong, Y.Y. Xu, Improving hydrophilicity and protein resistance of poly(vinylidene fluoride) membranes by blending with amphiphilichyper branched star polymer. Langmuir **23**, 5779–5786 (2007)
35. M. Khayet, M. Essalhia, M.R. Qtaishat, T. Matsuura, Robust surface modified
36. polyetherimide hollow fiber, membrane for long-term desalination by membrane distillation. Desalination **466**, 107–177 (2019)

Figures

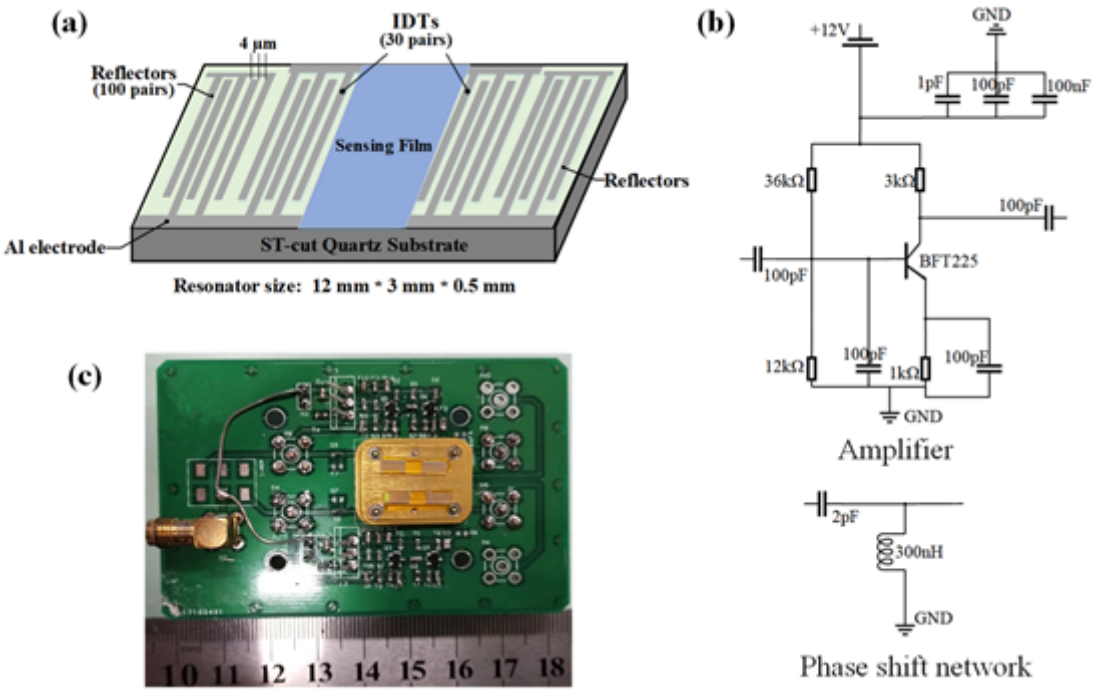

Figure 1

SAW sensor: (a) resonator structure diagram; (b) peripheral matching circuit diagram; (c) sample diagram.

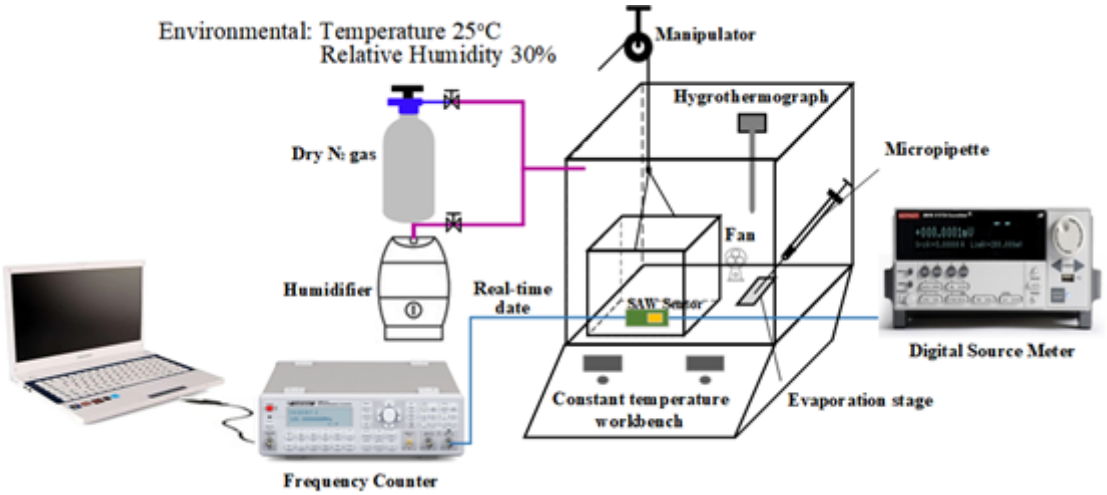

Figure 2

Schematic diagram of experimental sensing system.

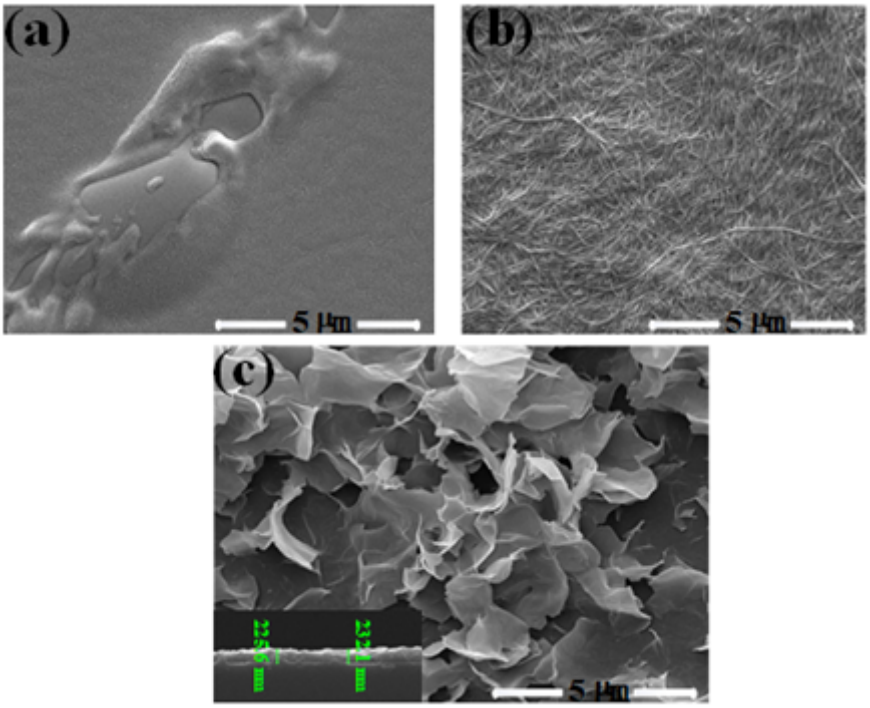

Figure 3

SEM image of (a) PEI nanofilm; (b) PEI/BC bi-layer nanofilms; and (c) ZIF-8@PEI/BC composite nanofilms.

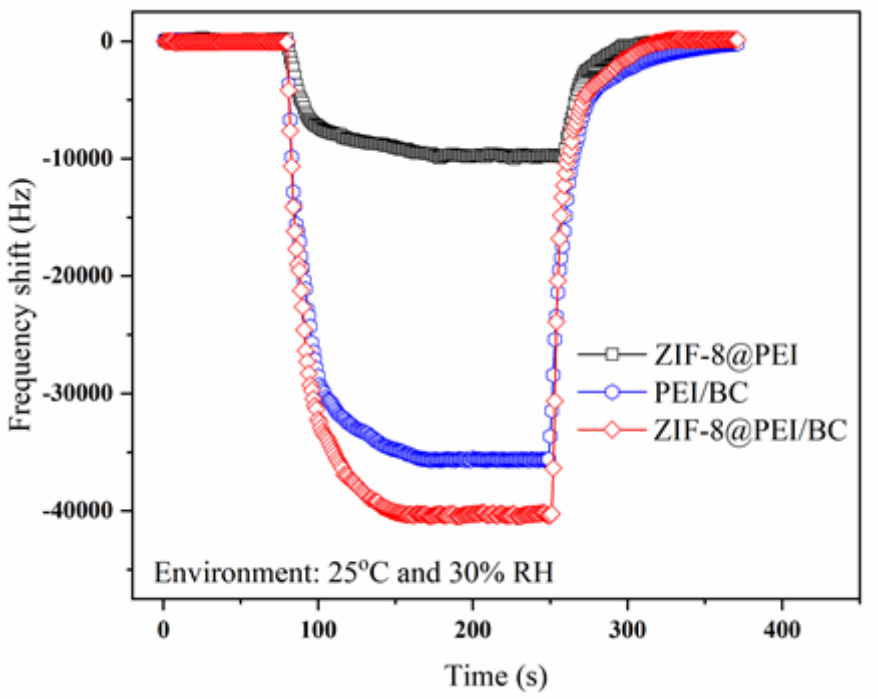

Figure 4

The response of ZIF-8@PEI nanofilms, PEI/BC bi-layer nanofilms and ZIF-8@PEI/BC composite nanofilms SAW sensor to 10 ppm formaldehyde gas under 25oC and 30% RH.

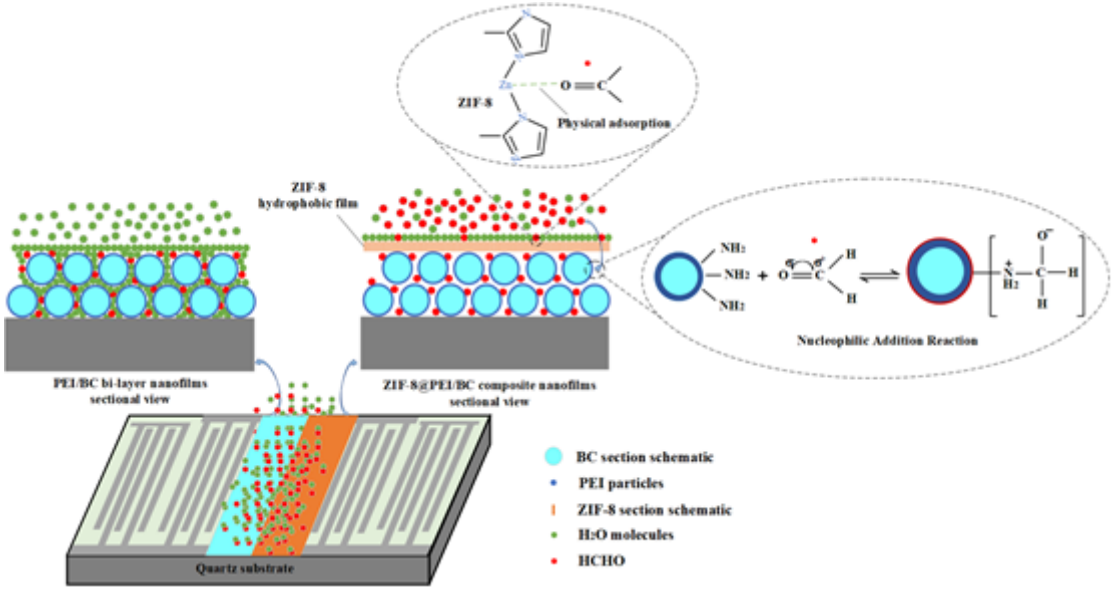

Figure 5

The mechanism diagram of PEI particles adsorbing formaldehyde molecules and the schematic diagram of ZIF-8 hydrophobic structure blocking water molecules from entering the pores of the film.

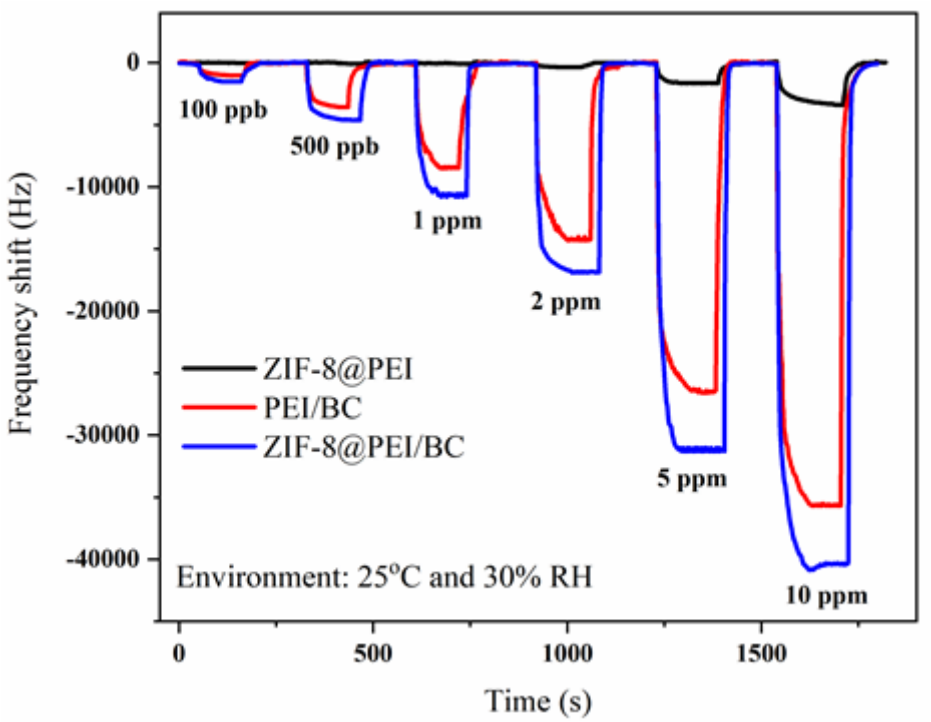

Figure 6

The response performance of ZIF-8@PEI nanofilms, PEI/BC bi-layer nanofilms [15] and ZIF-8@PEI/BC composite nanofilms to different low concentrations of formaldehyde gas under 25oC and 30% RH.

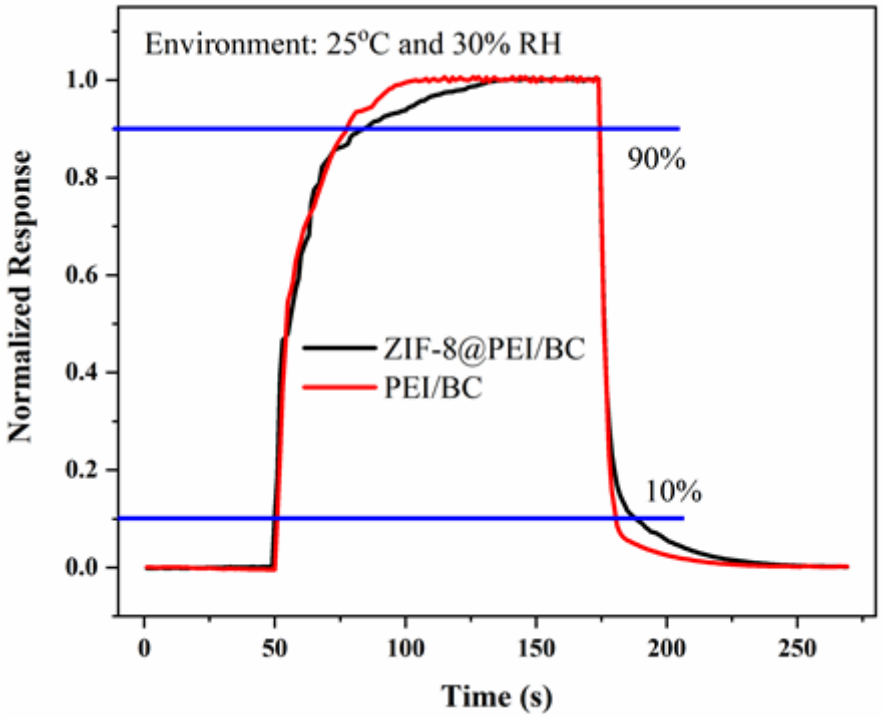

Figure 7

Normalized response/recovery curve of PEI/BC bi-layer nanofilms and ZIF-8@PEI/BC composite nanofilms to 10 ppm formaldehyde gas under 25oC and 30% RH.

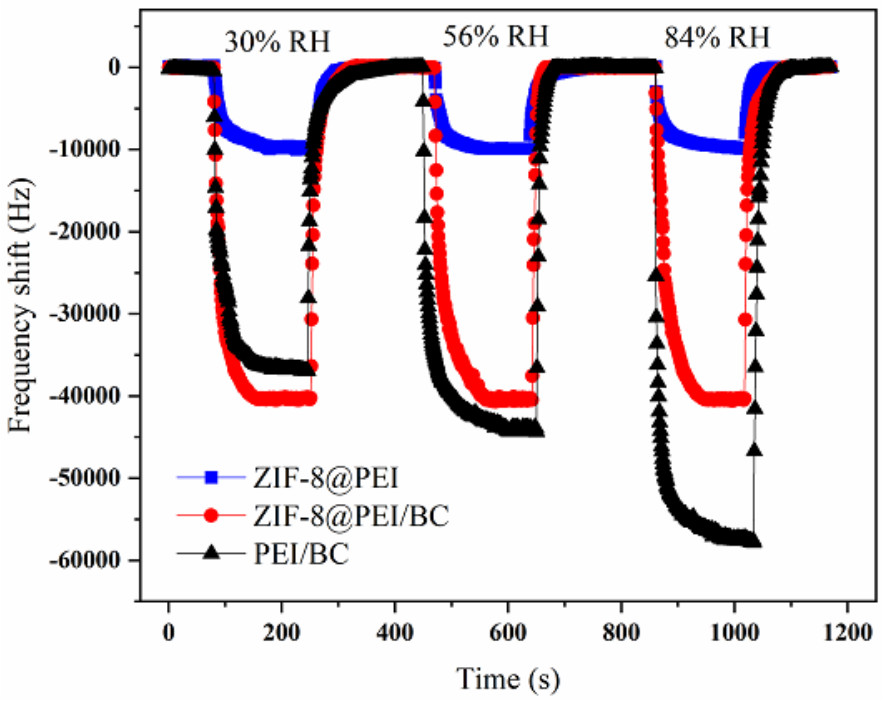

(a)

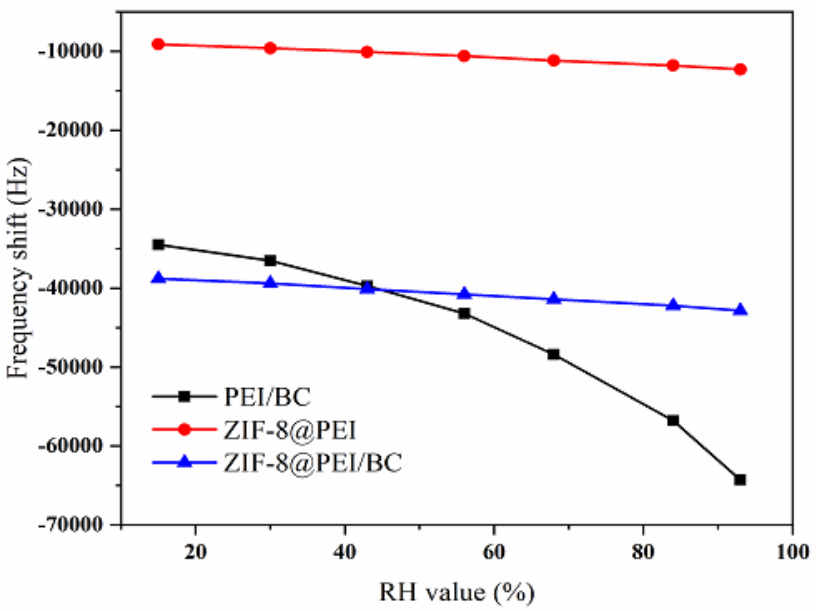

(b)

Figure 8

ZIF-8@PEI nanofilms, PEI/BC bi-layer nanofilms and ZIF-8@PEI/BC composite nanofilms SAW sensor: (a) response/recovery curves to 10 ppm formaldehyde gas under 30%, 56% and 84% humidity environmen; (b) result of frequency deviation of 10 ppm formaldehyde gas under 10%~93% humidity environment (keep the same room temperature at 25oC).

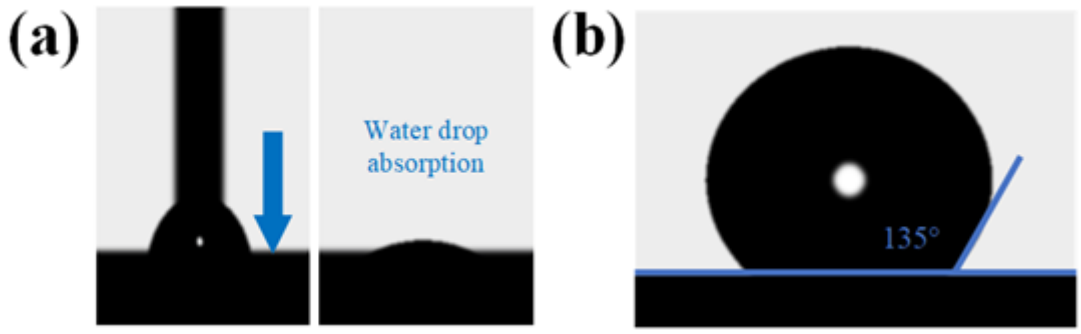

Figure 9

Water contact angle measurement of (a) PEI/BC nanofilms and (b) ZIF-8@PEI/BC composite nanofilms.

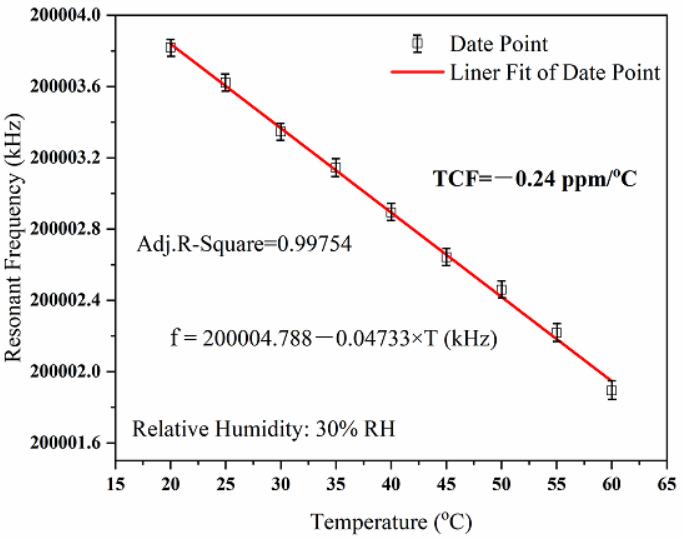

(a)

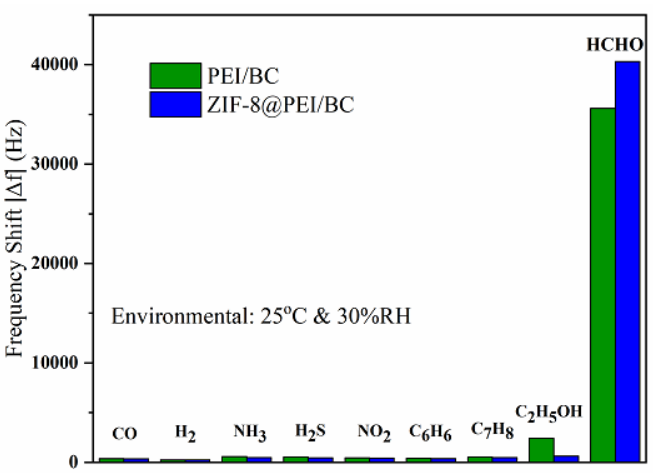

(c)

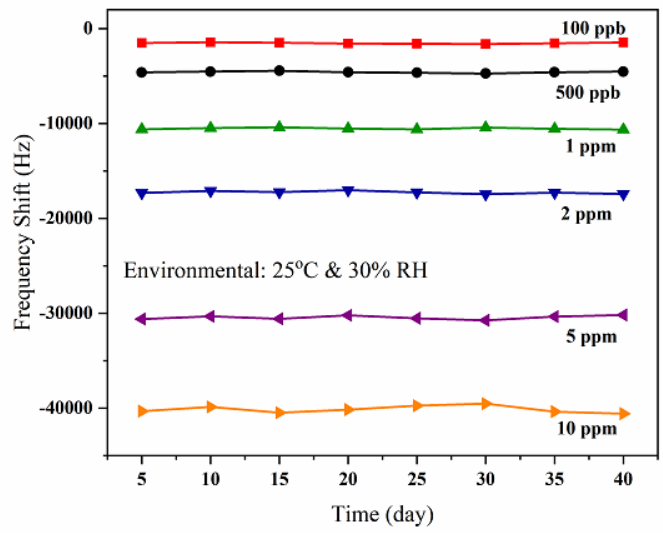

(b)

Figure 10

ZIF-8@PEI/BC composite nanofilms SAW sensor: (a) the relationship between resonance frequency and temperature; (b) repetitive detection of exposure to different concentrations of formaldehyde for 40 days; (c) with PEI/BC bi-layer nanofilms SAW sensor exposure to 100 ppm of various common industrial gases and 10 ppm of formaldehyde gas frequency shift, respectively.